Chromium chelated kappa carrageenan and its antibacterial activity

Saad Salman[1]
[1]Department of Pharmacy, The University of Lahore (Islamabad Campus)
saadirph@gmail.com

Introduction

Carrageenan (car-) are comprised of linear sulfated polysaccharides family isolated from the species of Rhodophyta (Patel 2012; Shukla et al. 2016). These polysaccharides and their derivatives have been exploited in cosmetics, food, and pharmaceuticals. Other beneficial activity of car- has been further explored in the drug delivery system as a controlled release agent that possess antioxidant properties as well (Genicot et al. 2018; Li et al. 2014). There are three variants of car- i.e. lambda, kappa, iota, and among them κ- possess peculiar range of properties such as biocompatibility, biodegradability, mechanical strength and hydrophilicity exploited in food industry as a stabilizing and thickening agent (Derkach et al. 2018; Ghanbarzadeh, Golmoradizadeh, and Homaei 2018; Sahiner, Sagbas, and Yılmaz 2017). Car- films in combination with glycerol and citric acid further ameliorate the anti-microbial activity (Khare et al. 2016; Sedayu, Cran, and Bigger 2019). While reliable bioassays are needed to recognize a wide range of pharmacological properties present in plants and their corresponding metal complexes. Chromium (Cr^{3+}) is a toxic metal and carcinogenic but its complexation with few ligands proves them to be a potential therapeutic agent. Cr^{3+} complexes with amino acid derivatives showed antimicrobial activity against different bacterial species. Antibiotics with ceftriaxone with metal complexes showed good antimicrobial properties. The complex of metals with 4-hydroxypyridine and azide ion Zn^{2+} complex with tridentate ligand showed low antibacterial but high antifungal properties.
The movement of Cr^{3+} in living organisms depends considerably on the complexation of the metal center by chelating nitrogen donor ligands. Cr^{3+} cysteine and hydrazide complexes, on the other hand, have noticeable antibacterial and antifungal activities. Sulfonamides, Sulfanilamide derivatives and cephapirin with Cr^{3+} complexes showed good antimicrobial properties. Monoamine oxidase-B inhibition by Cr^{3+} triethanolamine complexes leads to the prevention of some neurodegenerative diseases.
The activities of compounds obtained from plants and their metal complexes can be detected by the same conventional methods based on the same principle and are not equally efficient and sensitive. It is clear that biological evaluation, in general, can be carried out much more proficiently on water-soluble, nice crystalline complexes than on mixtures like plant exudate (Zaidi et al. 2012). However, the antibacterial activities of Cr^{3+} with κ, to the best of our knowledge, have not been reported yet.
Previously, we had studied the preparation and antimicrobial activity of nicotine and its Zn^{2+} complex. However, minimum inhibitory concentration (MIC) was the basis for the evaluation of the antibacterial activity. In this study, the complexed κ- *in-vitro* activity was evaluated against different types of pathogenic gram-negative and gram-positive bacteria.

MATERIALS AND METHODS

2.2. Computational Studies

The retrieval of ligand and corresponding bacterial proteins were conducted from PubChem and

Protein Data Bank (PDB). The well-known pathogenic strained proteins that were selected for the inhibitory activity prediction were 3zmi and 4urm. The structures obtained were refined with the help of ProDRG server and Modrefiner. PatchDock was then used for docking studies coupled with Discovery Studio 4.0 for the visualization of receptors and ligands.

2.3. Chromium Adsorption

The chromium was adsorbed in a batch mode at different pH while different isotherms were obtained through previously reported techniques. The adsorbed chromium was then subjected to antibacterial activity over various resistant strains.

2.4. Antibacterial Activity

K- with Cr^{3+} ion adsorbed were undergone antibacterial activity through "Agar Well diffusion Method". According to this method, the components of the dehydrated medium were weighed and dissolved in one liter of distilled water and heated up to boiling to dissolve the components completely. The medium was autoclaved at 121 °C keeping the pressure of 15 Ibs/in^2 for 15 minutes. After sterilization, the medium was then transferred to petri dishes and left for a few minutes so the components in the media should be solidified. It was then moved to incubator whose temperature was maintained at 37 °C and incubated for a day in order to look for any contamination occurred during the process. Those plates were selected which had no contaminations in it. This solution was prepared by concentrating the samples up to 1 mg/ml in di-methyl sulphoxide (DMSO) and other dilutions made from DMSO were 50 and 100 µg/ml respectively. Media used for this purpose was Mueller-Hinton is summarized in Table 1. The compounds were used in two concentrations i.e. at 50 µg/100 µl and 100 µg/100 µl.

One loop full of 24 hours of old bacterial culture containing approximately 104-106 CFU, was spread on the surface of agar plates. Autoclaved metallic borer was used to construct wells in the medium. The marked area was filled with diluted solutions of the test samples, metal salts, and solvent di-methyl sulphoxide. These plates were incubated at 37 °C for 24 hours. After this period, a clear zone of inhibition was seen which indicates anti-bacterial activity which was then used to measure in-vitro activity shown by the test compound. In our study, chromium sulfate and κ alone did not show any noticeable antibacterial activity. Figure 2 and 3 summarize all the results of the activity.

2.2. Test for acute toxicity

To conduct this test, the guidelines prescribed by OECD (Organization for Economic Cooperation and Development guideline) were followed. The test doses used in the animal model have a limit dosage of 2000 mg/kg. Six groups fasted for 3-4 hours, those female albino mice having a weight of 20-25 g were taken into account for the test. Then, the crude extract of Rhodophyta was administered in the doses of 1000-1500 mg/kg. Finally, the control group of these mice was administered with a dose of 2000 mg/kg. These mice were deprived of water and food for further 1-2 h. For the next 24 hours, these mice were checked for toxicity, mortality or aberrant behavioral changes such as coma, diarrhea, sedation, convulsions, or abnormal eating habits or breathing, alertness, restlessness, and other motor responses were evaluated.

RESULTS

3.2. Computational Studies

3.2.1. Activity prediction

The prediction analysis through Molinspiration studies showed that the Debilon (DN) and Phorbasterone-B demonstrates some good results for enzyme inhibition value of 0.28 and 0.32 whereas nuclear receptor ligand binding of 0.35 and 0.62 respectively as shown in Table 2. Bromo-indole on the other hand did not show enhanced activity for any of the bioactivity prediction analysis. This molecule was then tapered off for further docking and ADME properties and toxicity studies.

3.2.2. ADMET Properties

Through pKCSM and SwissADME, the ADME properties showed that PB has the solubility of -6.077 whereas for the DN it is -3.099 log mol/L. The value for the intestinal absorption is almost the same for both the molecules. PB is the only molecule having P-glycoprotein I as well as II inhibitor properties. It is the only molecule which is a CYP3A4 substrate. The ADME properties are given in Table 3. The bioavailability radar (Figure) as well as BOILED-egg approach (Figure 2) of both the molecules demonstrated low BBB penetration and low GIT absorption. It has also demonstrated low in-saturation and solubility, whereas high polarity, lipohilicity, size, and flexibility of the molecules. The red dot on the yolk showed that these molecules can be used for human body.

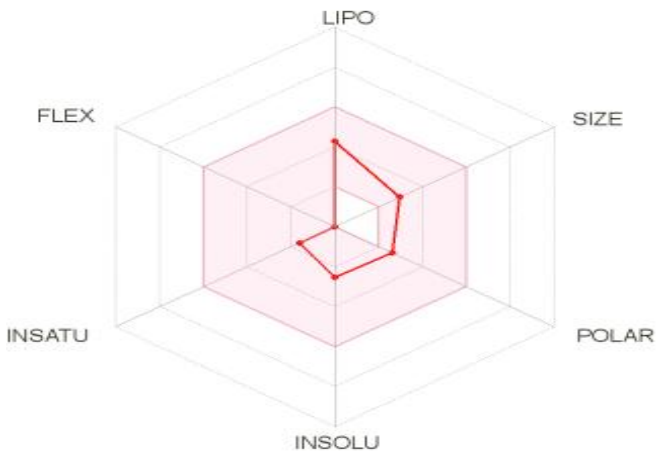

Figure 1: The bioavailability radar for the determination of the insaturation, solubility, polarity, lipohilicity, size, and flexibility of the molecules.

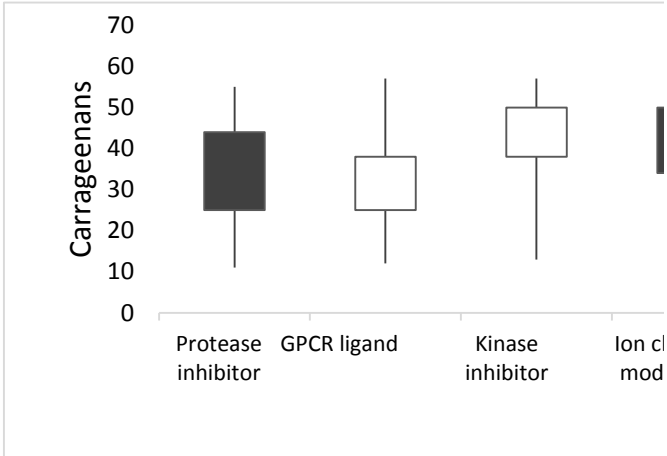

Table 2: The bioactivity predication analysis through Molinspiration analyzer.

3.2.3. Toxicity Analysis through computational approach

Gausar analyzer (http://www.pharmaexpert.ru/GUSAR/AcuToxPredict/) was used to predict the toxicity of these molecules. It analyzes the molecules on the basis of their toxicity while administering the following molecules through a specific route of administration and classification on the basis of OECD project as shown in Table 5. The results showed that the DN cannot be administered peritoneally with the LD50 log10 value of 0.574 mmol/kg whereas the PB had an oral toxic profile with the value of LD50 log10 of -0.391 mmol/kg. DN's applicability domain was in oral, subcutaneous and intravenous rat models. The PB's applicability domain for human consumption was peritoneal, intravenous and subcutaneous rat models. The results are shown in Table 5.

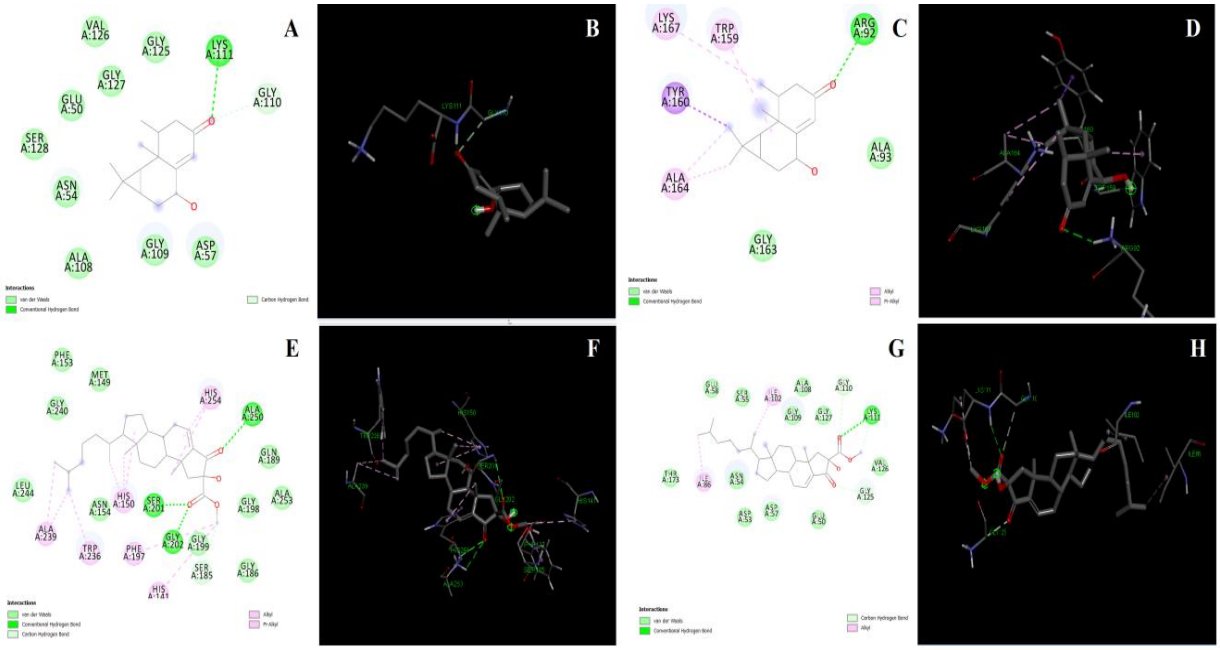

Rat model - IP (Intraperitoneal administration), Oral (Oral administration route), SC (Subcutaneous administration), IV (Intravenous administration), '-' (out of the domain of applicability), '+' (in the domain of applicability), LD50 (mmol/kg), LD50 (mg/kg), Cl (classification), where 5, 4, 3, 2, represent the classes.

3.2.4. Docking Results

The interaction energy of DN and PB with 3ZMI is -122.14 kj/mol and -116.78 kj/mol respectively whereas -128.19 kj/mol interaction energy of DN with 4URM whereas the interaction energy of -111.19 kj/mol of PB with 4urm. Both the molecules demonstrate Van der Waals interactions and C-H interaction. The amino-acid's non-covalent interaction with 4urm and 3zmi makes them a perfect candidate for the experimental studies.

Table 3: pKCSM prediction analysis for the ADME properties.

Model Name	**Unit**	**DN**	**PB**
		Predicted Value	**Predicted Value**
ABSORPTION			
Water solubility		-3.099	-6.077
Caco2 permeability	log Papp in 10 cm/s	1.433	0.508
Intestinal absorption	% absorbed	95.762	95.956
Skin Permeability	log Kp	-3.073	-3.103
P-glycoprotein I inhibitor	Yes/No	No	Yes
P-glycoprotein II inhibitor	Yes/No	No	Yes
DISTRIBUTION			
VDss (human)	log L/kg	0.341	-0.197
Fraction unbound (human)	Fu	0.392	0
BBB permeability	log BB	0.426	0.175
CNS permeability	log PS	-2.634	-1.916
EXCRETION			
Model Name	**Unit**	**Predicted Value**	**Predicted Value**
Total Clearance	log ml/min/kg	0.922	0.495
Renal OCT2 substrate	Categorical	No	No
METABOLISM			
CYP2D6 substrate	Categorical	No	No
CYP3A4 substrate	Categorical	No	Yes
TOXICITY			
AMES toxicity	Categorical	No	No
Max. tolerated dose (human)	log mg/kg/day	0.176	-0.485
Oral Rat Acute Toxicity (LD50)	mol/kg	1.7	2.148
Oral Rat Chronic Toxicity (LOAEL)	log mg/kg bw/day	1.729	2.122
Hepatotoxicity	Categorical	No	No
Skin Sensitization	Categorical	Yes	No
T.Pyriformis toxicity	log ug/L	0.941	0.371
Minnow toxicity	log mM	1.683	y -1.495

Table 4: The SwissADME prediction analysis for the ADME properties.

Physicochemical Properties			**Pharmacokinetics**		
Properties	**DN**	**PB**	**Properties**	**DN**	**PB**
Formula	$C_{15}H_{22}O_2$	$C_{43}H_{64}O_6$	GI absorption	High	Low
MW	234.33 g/mol	676.96 g/mol	BBB permeant	Yes	No
No. heavy atoms	17	49	P-gp substrate	No	Yes
Heavy atoms	0	0	CYP1A2 inhibitor	No	No
Fraction Csp^3	0.80	0.84	CYP2C19 inhibitor	No	No
Rotatable bonds	0	5	CYP2C9 inhibitor	No	No
H-acceptors	2	6	CYP2D6 inhibitor	No	No
H-bond donors	1	2	TPSA	37.30 Å²	100.90 Å
Molar Refractivity	68.24	196.08	Log *K*p (skin permeation)	-6.32 cm/s	-4.05 cm/s
Lipophilicity			**Drug-likeness**		
iLOGP	2.36	5.19	Lipinski	Yes; 0 violation	No; 2 violations: MW>500, MLOGP>4.15
XLOGP3	1.98	8.98	Ghose	Yes	No; 4 violations: MW>480,WLOGP>5.6, MR>130, #atoms>70
WLOGP	2.56	8.04	Veber	Yes	Yes
MLOGP	2.63	5.36	Egan	Yes	No; 1 violation: WLOGP>5.88
SILICOS-IT	2.67	7.18	Muegge	Yes	No; 2 violations: MW>600, XLOGP3>5
Log $P_{o/w}$	2.44	6.95	Bioavailability Score	0.55	0.17
Water Solubility			**Medicinal Chemistry**		
Solubility Class	6.75e-01 mg/ml ; 2.88e-03 mol/l Soluble	2.92e-07 mg/ml ; 4.32e-10 mol/l Poorly soluble	Brenk	0 alert	Beta-keto anhydride isolated alkene
			Leadlikeness	1 violation: MW<250	2 violations: MW>350, XLOGP3>3.5
			Synthetic accessibility	4.21	9.04
Solubility Class	9.57e-01 mg/ml ; 4.08e-03 mol/l Soluble	6.95e-09 mg/ml ; 1.03e-11 mol/l Insoluble	Log *S* (Ali)	-2.39	-10.99
			Solubility Class	5.83e-01 mg/ml ; 2.49e-03 mol/l **Soluble**	1.31e-05 mg/ml ; 1.94e-08 mol/l **Poorly soluble**
Log *S* (SILICOS-IT)	-2.60	7.71			

The docking studies of κ has been reported elsewhere. The docking studies of κ demonstrated very good interaction with 4URM and 3, hence confirming the antibacterial activity against gram positive and gram-negative bacterial strains. The results are shown in Figure. The results showed that maximum Cr^{3+} ions were adsorbed at the pH of 6. Whereas, the pH of the system raised the sorption of Cr^{3+} ions from pH 3 to pH 6 and then suddenly started declining at pH 7-9. The pH effect on the Cr^{3+} ion percentage adsorption has been shown in Figure 1.

S	**Dubinin-Radushkevich**			**Freundlich**		
	qs/mg g^{-1}	**E**	**R^2**	**K$_F$/mg g^{-1}**	**n**	**R^2**
κ	36.71	2.21k	9.812	11.54	0.61	0.941
DN	21.67	4.11k	9.921	10.25	0.21	0.892
PB	28.32	5.31k	9.933	13.21	0.53	0.979

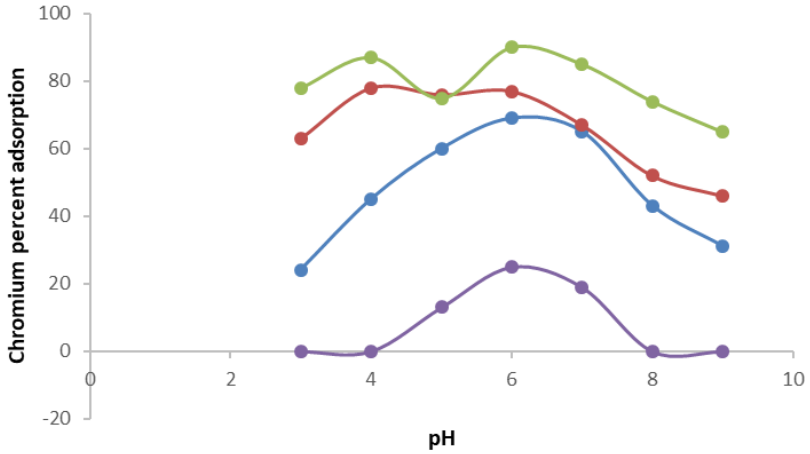

Figure 1: The pH effect on Cr^{3+} ions over κ.

The Freundlich and Dubinin-Radushkevich in Figure 2 and Figure 3 best explains the adsorption of Cr^{3+} ions. Both the models fitted the most for the adsorption of Cr^{3+} ions.

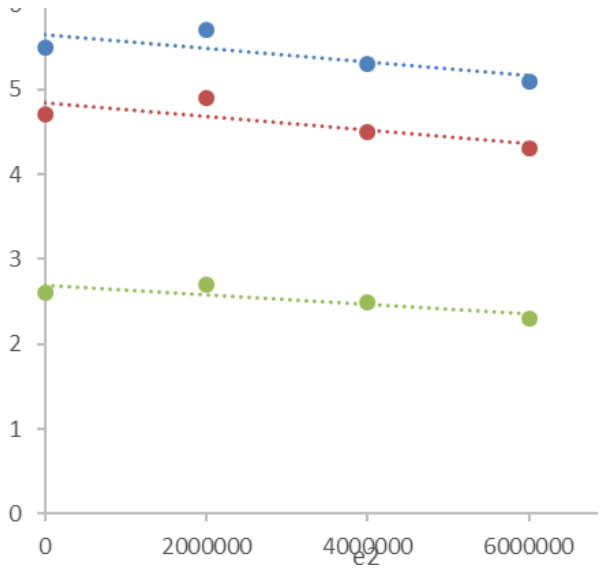

Figure 2: Antibacterial activities of κ and Cr^{3+} complex over gram-positive and negative species at a dose of 50 µg/100 µl.

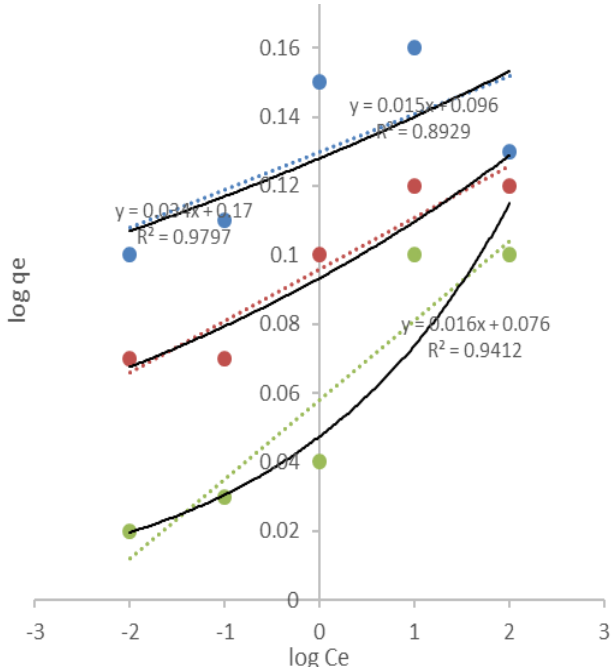

Figure 2: The Freundlich model of sorption for Cr^{3+} ions over three different dosages. A) The green dotted line represents the 10ppm solution of Cr^{3+} ions. B) The red dotted line represents the 20 ppm solution of Cr^{3+} ions whereas; the C) blue dotted line represents the 25 ppm of the Cr^{3+} ions solution.

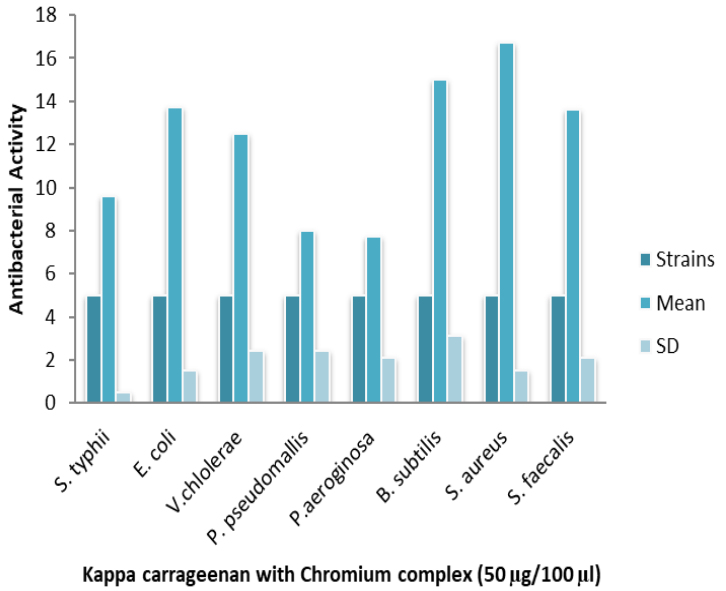

Figure 2: Antibacterial activities of κ and Cr^{3+} complex over gram-positive and negative species at a dose of 50 µg/100 µl.

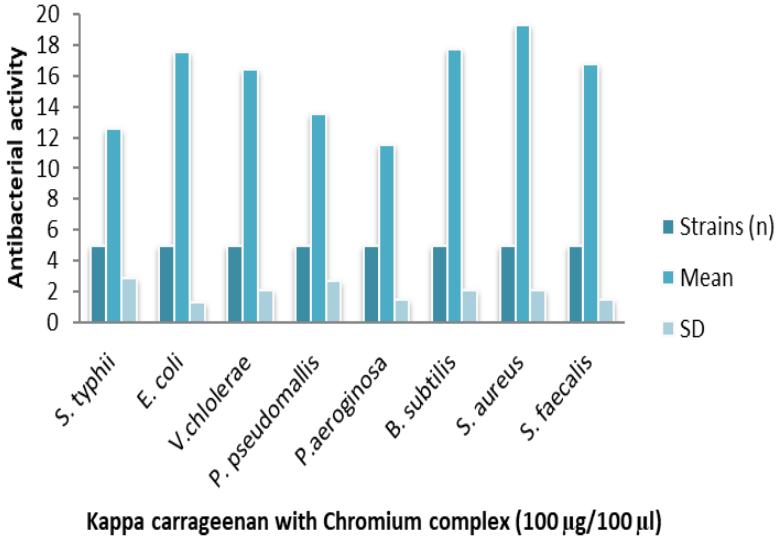

Figure 3: Antibacterial activities of κ- and Cr^{3+} complex over gram-positive and negative species at a dose of 100 µg/100 µl.

3.2. Acute toxicity evaluation through experiment

It was revealed from the studies that at 2000 mg/kg, no mortality rate was observed. That may also suggest that the LD50 value could be larger than these concentrations. Also, at the dose of 1000 and 1500 mg/kg, no signs of mortality or toxicity. And for the next 24 hours, these mice did not demonstrate any aberrant behavioral changes such as coma, diarrhea, sedation, convulsions, or abnormal eating habits or breathing, alertness, motor response or restlessness.

CONCLUSION

κ and their adsorbed Cr^{3+} complexes possess excellent proficiency by hindering the growth of pathogenic strains of bacteria at the higher dose level. Computational outcomes revealed that DN and PB compounds are very active and have maximum solubility in the intestine but poor blood-brain

barrier penetration. Rhodophyta extracts demonstrated alkaloids, polyphenols, saponins, tannins, steroids, flavonoids, and terpenoids. Whereas the Freundlich and D-R models have proven efficient adsorption of Cr^{3+} over κ. Docking studies proved bacterial proteins are inhibited by these molecules. The toxicity studies and prediction analysis had demonstrated good results for human consumption. Due to this very reason, these compounds could be used as broad-spectrum antibacterial agents.

REFERENCES

Derkach, S. R., N. G. Voron'ko, Yu. A. Kuchina, D. S. Kolotova, A. M. Gordeeva, D. A. Faizullin, Yu. A. Gusev, Yu. F. Zuev, and O. N. Makshakova. 2018. "Molecular Structure and Properties of κ-Carrageenan-Gelatin Gels." Carbohydrate Polymers 197:66–74.

Genicot, Sabine, Aurélie Préchoux, Gaëlle Correc, Nelly Kervarec, Gaëlle Simon, and James S. Craigie. 2018. Carrageenans: New Tools for New Applications. Blue Biotechnology.Ghanbarzadeh, Mehri, Asma Golmoradizadeh, and Ahmad

Homaei. 2018. Carrageenans and Carrageenases: Versatile Polysaccharides and Promising Marine Enzymes. Phytochemistry Reviews 17(3):535–71.

Khare, Anshul Kumar, Robinson J. J. Abraham, V. Appa Rao, and R. Narendra Babu. 2016. Utilization of Carrageenan, Citric Acid and Cinnamon Oil as an Edible Coating of Chicken Fillets to Prolong Its Shelf Life under Refrigeration Conditions. Veterinary World 9 (2):166–75.

Li, Liang, Rui Ni, Yang Shao, and Shirui Mao. 2014. Carrageenan and Its applications in Drug Delivery. Carbohydrate Polymers 103:1–11.

Patel, Seema. 2012. Therapeutic Importance of Sulfated Polysaccharides from Seaweeds: Updating the Recent Findings. Biotech 2(3):171–85.

Sahiner, Nurettin, Selin Sagbas, and Selahattin Yılmaz. 2017. Microgels Derived from Different Forms of Carrageenans, Kappa, Iota, and Lambda for Biomedical Applications. MRS Advances 2 (47): 2521–27.

Sedayu, Bakti B., Marlene J. Cran, and Stephen W. Bigger. 2019. A Review of Property Enhancement Techniques for Carrageenan-Based Films and Coatings. Carbohydrate Polymers 216:287–302.

Shukla, Pushp S., Tudor Borza, Alan T. Critchley, and Balakrishnan Prithiviraj. 2016. Carrageenans from red seaweeds as promoters of growth and elicitors of defense response in plants. Frontiers in Marine Science 3:81.